Polarization phenomena in open charm photoproduction processes

Egle Tomasi-Gustafsson*
DAPNIA/SPhN, CEA/Saclay, 91191 Gif-sur-Yvette Cedex, France

Michail P. Rekalo†
Middle East Technical University, Physics Department, Ankara 06531, Turkey
(Received 10 November 2003; published 20 May 2004)

We analyze polarization effects in the associative photoproduction of pseudoscalar ($\bar{D}_c$) charmed mesons in exclusive processes $\gamma+N\to Y_c+\bar{D}_c$, $Y_c=\Lambda_c^+$, Σ_c. Circularly polarized photons induce nonzero polarization of the Y_c hyperon with x and z components (in the reaction plane) and nonvanishing asymmetries $\mathcal{A}_x$ and $\mathcal{A}_z$ for polarized nucleon targets. These polarization observables can be predicted in a model-independent way for the exclusive $\bar{D}_c$-production processes in collinear kinematics. The T-even components of the Y_c-polarization and asymmetries for noncollinear kinematics can be calculated in the framework of an effective Lagrangian approach. The depolarization coefficients D_{ab}, characterizing the dependence of the Y_c polarization on the nucleon polarization, are also calculated.

DOI: 10.1103/PhysRevD.69.094015 PACS number(s): 13.88.+e, 13.40.−f, 14.40.Lb, 14.65.Dw

I. INTRODUCTION

The experimental study of the photoproduction of charmed particles on nucleons through the exclusive and inclusive reactions $\gamma+N\to Y_c+\bar{D}_c$ ($\bar{D}_c^*$), $Y_c=\Lambda_c(\Sigma_c)$, $\gamma+N\to N+D_c+\bar{D}_c$, $\gamma+N\to\Lambda_c(\bar{\Lambda}_c)+X$, etc., started about 20 years ago [1,2] in the photon energy range $E_\gamma=20-70$ GeV. Since then, several experiments have been devoted to this subject [3–6], but up to now, the smallest energy where data are available has been $E_\gamma=20$ GeV [3], which is still relatively far from threshold (for example, $E_{thr}=8.7$ GeV for $\gamma+p\to\Lambda_c^++\bar{D}^0$).

Charm particle photoproduction is usually interpreted according to the photon-gluon fusion (PGF) mechanism $\gamma+G\to c+\bar{c}$ [7], which can be considered as the simplest QCD hard process [called the leading order (LO) approximation].

Considering the corresponding fragmentation functions for $c\to D_c+X$, $c\to Y_c+X$, $c\to\bar{D}_c+X$, ..., the observables for inclusive processes of charmed mesons and hyperons photoproduction can be calculated. The existing experimental data on the total cross section for open charm photoproduction, $\gamma+N\to\text{charm}+X$, the relative production of D^0 and D^+ mesons as well as Λ_c^+ hyperons can be explained within this approach.

In principle, other mechanisms (of nonperturbative nature) should also be taken into account, such as, for example, the diffractive production of $D_c\bar{D}_c$ or Λ_cD_c pairs, through Pomeron exchange. Different hadronic exchanges can also contribute to the simplest exclusive processes $\gamma+N\to Y_c+\bar{D}_c$ ($\bar{D}_c^*$) in the near-threshold region [8,9]. More experimental and theoretical studies are certainly needed in order to clarify the physics of charm particle photoproduction.

Up to now, all charm photoproduction experiments have been done with unpolarized particles.[1] Polarization phenomena will be essential for the understanding of the reaction mechanism, in particular of the importance of the main subprocess $\gamma+G\to c+\bar{c}$. For example, T-even polarization observables such as the Σ_B asymmetry [10], induced by a linearly polarized photon beam, the asymmetries in collisions of circularly polarized photons on polarized gluons [11], and the polarization of the c quark have relatively large absolute values, in the framework of this model and can be actually measured. The running COMPASS experiment [12], with longitudinally polarized muons and polarized targets (p or LiD), will access these polarization effects.

High-energy photon beams with a large degree of circular polarization are actually available for physical experiments. Complementary to the linear polarized photon beams, they allow one to address different interesting problems of hadron electrodynamics. Circularly polarized photon beams can be obtained in different ways—for example, by backward scattering of a laser beam by high-energy electron beam with longitudinal polarization. In JLab circularly polarized bremsstrahlung photons were generated by polarized electrons [13,14]. The proton polarization in the process of deuteron photodisintegration, $\vec{\gamma}+d\to\vec{p}+n$ [15], was investigated to test QCD applicability [16], with respect to hadron helicity conservation in high-energy photon-deuteron interactions. Coherent scattering of a longitudinally polarized electron beam by a diamond crystal results in a very particular beam of circularly polarized photons [17]. In the COMPASS experiment [12], the high-energy longitudinally polarized muon beam generates circularly polarized photons (real and virtual) in a wide energy interval (50–130 GeV).

The interest in a circularly polarized photon beam is re-

*Electronic address: etomasi@cea.fr
†Permanent address: NSC Kharkov Institute of Physics and Technology, 61108 Kharkov, Ukraine.

[1]We should mention here an earlier attempt [3] to study open charm photoproduction with linearly polarized photons.

lated to the very actual question about how the proton spin is shared among its constituents [18–21]. The determination of the gluon contribution ΔG to nucleon spin is the object of different experiments with polarized beams and targets [22,23].

In particular, the production of charmed particles in the collision of longitudinally polarized muons with a polarized proton target will be investigated by the COMPASS Collaboration. In the framework of the photon-gluon fusion model [7], $\gamma^*+G\to c+\bar{c}$ (γ^* is a virtual photon), the corresponding asymmetry (for polarized μp collisions) is related to the polarized gluon content in the polarized protons [24–26]. As a result of the future impact of such a result, it seems necessary to understand all other possible mechanisms which can contribute to inclusive charm photoproduction, such as $\gamma+p\to\bar{D}^0+X$, for example. One possible and *a priori* important background, which can be investigated in detail, is the process of exclusive associative charm photoproduction, with pseudoscalar and vector charmed mesons in the final state, $\gamma+p\to Y_c+\bar{D}_c(\bar{D}_c^*)$. The mechanism of photon-gluon fusion, which successfully describes the inclusive spectra of D and D^* mesons at high photon energies, cannot be easily applied to exclusive processes, at any energy. Threshold considerations of such processes in terms of standard perturbative QCD have been applied only to the energy dependence of the cross section of $\gamma+p\to p+J/\psi$ [27], as, in such approach, polarization phenomena cannot be calculated without additional assumptions.

In this respect, the formalism of the effective Lagrangian approach (ELA) seems very convenient for the calculation of the exclusive associative photoproduction of charmed particles, such as $\gamma+N\to Y_c^+\bar{D}_c(\bar{D}_c^*)$ [8,9,28], at least in the near-threshold region. Such an approach is also widely used in the analysis of various processes involving charmed particles [29], such as, for example, J/ψ suppression in high-energy heavy ion collisions, in connection with quark-gluon plasma transitions [30]. We analyzed earlier different exclusive processes of associative charm particles photoproduction, $\gamma+N\to Y_c^++\bar{D}_c(\bar{D}_c^*)$, in the threshold region, and indicated that polarization phenomena can be naturally predicted for those reactions. In this paper we extend this model to higher energies by including the mechanism of D_c^* exchange and apply the ELA to the collision of circularly polarized photons with an unpolarized and a polarized proton target. We predict the angular and energy dependences of the asymmetries in $\vec{\gamma}+\vec{N}\to Y_c^++\bar{D}_c$ processes and of the polarizations of the Y_c^+ hyperons, produced in $\vec{\gamma}+N\to Y_c^++\bar{D}_c$ with circularly polarized photons (on a polarized target) and in $\gamma+\vec{N}\to Y_c^++\bar{D}_c$ (with unpolarized photons on a polarized target).

The exclusive reactions $\gamma+N\to Y_c+\bar{D}_c$ ($\bar{D}_c^*$), which are the object of this paper, are important not only as possible background for experiments aiming at the measurement of the gluon contribution to the nucleon spin, but these processes have an intrinsic physical interest, in the understanding of charm particle electrodynamics. Let us mention some important aspects:

(i) the possibility to measure the electromagnetic properties of charmed particles, such as the magnetic moments of Y_c hyperons or the vector D^* meson;
(ii) a test of SU(4) symmetry for the strong ND_cY_c-coupling constants;
(iii) determination of the P parity of charmed particles;
(iv) explanation of the asymmetric ratio $D/\bar{D}_c$, $\bar{\Lambda}_c/\Lambda_c$ in open charm photoproduction reactions;
(v) understanding of nonperturbative mechanisms for associative charm photoproduction.

The reactions $\gamma+N\to Y_c+\bar{D}_c$ ($\bar{D}_c^*$) contribute to the total cross section, in particular in the near-threshold region, similarly to the processes of vector meson production, K and K^* production in πN or NN collisions. For example, at $E_\gamma=20$ GeV, the associative $\Lambda_c\bar{D}_c$ production contributes for 71% to the total cross section of open charm photoproduction [3].

The paper is organized as follows. Using the standard parametrization of the spin structure for the matrix element of $\gamma+N\to Y_c+\bar{D}_c$ processes, in Sec. II we calculate the single- and double-spin polarization observables in terms of four scalar amplitudes. Sections III and IV contain a description of possible nonperturbative mechanisms for exclusive associative charm photoproduction and the relativistic parametrization of the corresponding matrix elements. In Sec. V we give three sets of parameters, corresponding to three possible models for $\gamma+p\to\Lambda_c^++\bar{D}^0$, which describe the energy dependence of the total cross section. Polarization phenomena for the three models are discussed in Sec. VI. The expressions for the scalar amplitudes f_i, corresponding to the different diagrams, are given in the Appendix.

II. POLARIZATION OBSERVABLES FOR $\gamma+N\to Y_C+\bar{D}_C$

We consider here different polarization observables for associative $Y_c\bar{D}_c$ photoproduction, starting from the simplest single-spin asymmetry Σ_B, induced by photons with linear polarization, to the depolarization coefficients $\mathcal{D}_{ab}$, which describe the dependence of the polarization of the produced Y_c hyperon on the nucleon target polarization.

A. Spin structure of the matrix element and differential cross section

We will use the standard parametrization [31] of the spin structure for the amplitude of pseudoscalar meson photoproduction on the nucleon:

$$\mathcal{M}(\gamma N\to Y_c\bar{D}_c)=\chi_2^\dagger[i\vec{\sigma}\cdot\vec{e}f_1+\vec{\sigma}\cdot\hat{\vec{q}}\vec{\sigma}\cdot\hat{\vec{k}}\times\vec{e}f_2+i\vec{e}\cdot\hat{\vec{q}}\vec{\sigma}\cdot\hat{\vec{k}}f_3+i\vec{\sigma}\cdot\hat{\vec{q}}\vec{e}\cdot\hat{\vec{q}}f_4]\chi_1, \quad (1)$$

where $\hat{\vec{k}}$ and $\hat{\vec{q}}$ are the unit vectors along the three-momentum of γ and $\bar{D}_c$; f_i, $i=1-4$, are the scalar amplitudes, which are functions of two independent kinematical variables, the square of the total energy s and $\cos\vartheta$, where ϑ is the $\bar{D}_c$-meson production angle in the reaction center of

mass (c.m.) with respect to the direction of the incident photon, and χ_1 and χ_2 are the two-component spinors of the initial nucleon and the produced Y_c baryon.

Note that the pseudoscalar nature of the $\bar{D}_c$ meson has not been experimentally confirmed up to now; therefore, we follow here the prescription of the quark model for the P parities of $\bar{D}_c$ and Y_c-charm particles.

The differential cross section when all particles are unpolarized can be derived from Eq. (1):

$$\frac{d\sigma}{d\Omega}=\frac{q}{k}\frac{(E_1+m)(E_2+M)}{64\pi^2 s}\mathcal{N}_0$$

and

$$\mathcal{N}_0=|f_1|^2+|f_2|^2-2\cos\vartheta\,\mathrm{Re}\,f_1 f_2^*+\sin^2\vartheta\left\{\frac{1}{2}(|f_3|^2+|f_4|^2)+\mathrm{Re}[f_2 f_3^*+2(f_1+\cos\vartheta f_3)f_4^*]\right\}, \quad (2)$$

where $E_1(E_2)$ and $m(M)$ are the energy and mass of $N(Y_c)$, respectively, $k=\sqrt{E_1^2-m^2}$, and $q=\sqrt{E_2^2-M^2}$.

B. Charm photoproduction with linearly polarized photons

A linearly polarized photon beam on an unpolarized proton target may induce a beam asymmetry Σ_B defined as

$$\Sigma_B=\frac{d\sigma_\perp/d\Omega-d\sigma_\parallel/d\Omega}{d\sigma_\perp/d\Omega+d\sigma_\parallel/d\Omega}, \quad (3)$$

with

$$\mathcal{N}_0\Sigma_B=-\frac{\sin^2\vartheta}{2}[|f_3|^2+|f_4|^2+2\,\mathrm{Re}\,f_2 f_3^*+2\,\mathrm{Re}(f_1+\cos\vartheta f_3)f_4^*], \quad (4)$$

where $d\sigma_\perp/d\Omega$ and $d\sigma_\parallel/d\Omega$ are the differential cross sections for the absorption of photons with linear polarization, which is orthogonal or parallel to the reaction plane.

The measurement of this observable for the processes $\vec{\gamma}+N\to Y_c+\bar{D}_c$ is important as these reactions constitute a possible background with respect to PGF, $\vec{\gamma}+G\to c+\bar{c}$. For all these processes, Σ_B is the simplest polarization observable of T-even nature which does not vanish in the LO approximation. Moreover, for $\vec{\gamma}+G\to c+\bar{c}$, it has a large sensitivity to the mass of the c quark, as it is proportional to m_c^2 and it does not depend on the fragmentation functions $c\to D_c(\Lambda_c)+X$. In this approach, $\Sigma_B(\vec{\gamma}N\to c\bar{c}X)$ is determined by the unpolarized gluon distribution $G(x)$, which is relatively well known, in comparison with the polarized gluon distribution $\Delta G(x)$. So, in principle, $\Sigma_B(\vec{\gamma}N\to c\bar{c}X)$ can be predicted with better precision than the asymmetry $A_z(\vec{\gamma}\vec{N}\to c\bar{c}X)$ (in the collision of circularly polarized photons with a longitudinally polarized target) which is actually considered the most direct way to access $\Delta G(x)$.

High-energy photon beams with linear polarization can be obtained at SLAC and at CERN. In the conditions of the COMPASS experiment, the scattering of muons, $p(\mu,\mu'\bar{D}_c)X$, allows one, in principle, to measure Σ_B even for $Q^2\neq 0$. For this aim, it is necessary to study the ϕ dependence of the corresponding exclusive cross section, taking into account that the $\cos 2\phi$ contribution is proportional to Σ_B (where ϕ is the azimuthal angle of $\bar{D}_c$ production, with respect to the muon scattering plane).

C. Collisions of circularly polarized photons with a polarized proton target

Circularly polarized photon beams allow one to obtain additional dynamical information in comparison with photons with linear polarization, in hadronic processes (photoproduction or photodisintegration). The difference between linear and circular photon polarizations is due to the P-odd nature of the photon helicity ($\lambda=\pm 1$), which is the natural characteristic of circularly polarized photons. Therefore, in any binary process $\gamma+a\to b+c$ (a, b, and c are hadrons and/or nuclei), with circularly polarized photons, the asymmetry, in the case of unpolarized targets, vanishes, due to the P invariance of the electromagnetic interactions of hadrons. In contrast, linearly polarized photons generally induce nonzero asymmetry, even in the case of unpolarized targets and unpolarized final particles. Circular polarization manifests itself only in double-spin (or more) polarization phenomena, such as, for example, the correlation polarization coefficients of photon beams and proton targets, $\vec{\gamma}+\bar{p}\to\vec{\Lambda}_c^+ +\bar{D}_c^0$, or the polarization of the final Λ_c hyperon in $\vec{\gamma}+p\to\vec{\Lambda}_c^+ +\bar{D}_c^0$. Analysis of these processes is the object of the present paper. Note that in both cases the components of the target polarization and the Λ_c^+ polarization lie in the reaction plane, due to the P invariance. Note also that all these polarization observables are T even; i.e., they may not vanish even if the amplitudes of the considered process are real functions of kinematical variables.

Another possible double-spin correlation coefficient with circularly polarized photons for the process $\vec{\gamma}+p\to\Lambda_c^+ +\bar{D}^{*0}$ is the vector polarization of the D_c^* meson. In this connection, however, it is necessary to stress that the vector polarization of D_c^* cannot be measured through its most probable decays $D_c^*\to D_c+\pi$, $D_c^*\to D_c+\gamma$, $D_c^*\to D_c+e^+ +e^-$, which are induced by P-invariant strong and electromagnetic interactions. The matrix elements for these decays are characterized by a single-spin structure, which is insensitive to the vector polarization.

For completeness, let us mention two recent applications of high-energy circularly polarized photon beams. One is the experimental verification of the Gerasimov-Drell-Hearn sum rule [32], which is determined by an integral over the difference of the total $\vec{\gamma}\vec{N}$ cross section, with two possible total spin projections 3/2 and 1/2. Such a quantity $\sigma_{3/2}-\sigma_{1/2}$ can be measured in collisions of circularly polarized photons with a polarized nucleon target. Measurements are going on at MAMI for $E_\gamma<800$ MeV [33] and at JLab [34].

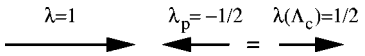

FIG. 1. Conservation of helicity in $\vec{\gamma}+\vec{p}\to\Lambda_c+D^0$ in the collinear regime.

In the general case, any reaction $\vec{\gamma}+\vec{p}\to Y_c+\overline{D_c^0}(\overline{D_c^*})$ (with circularly polarized photons and polarized target) is described by two different asymmetries, so the dependence of the differential cross section on the polarization states of the colliding particles can be parametrized as follows[2] (taking into account the P invariance of the electromagnetic interaction of charmed particles):

$$\frac{d\sigma}{d\Omega}(\vec{\gamma}\vec{p})=\left(\frac{d\sigma}{d\Omega}\right)_0(1-\lambda\mathcal{T}_x\mathcal{A}_x-\lambda\mathcal{T}_z\mathcal{A}_z), \tag{5}$$

where $\lambda=\pm1$ is the photon helicity, $\mathcal{T}_x$ and $\mathcal{T}_z$ are the possible components of the proton polarization $\vec{\mathcal{T}}$, and $\mathcal{A}_x$ and $\mathcal{A}_z$ are the two independent asymmetries. As a result of the T-even nature of these asymmetries, they are nonvanishing in the ELA, where the photoproduction amplitudes f_i are real. These asymmetries are nonzero also for hard QCD processes such as PGF, $\gamma+G\to c+\overline{c}$, for collisions of polarized photons and gluons with definite helicities [11].

After summing over the Y_c polarizations, one finds the following expressions for the asymmetries $\mathcal{A}_x$ and $\mathcal{A}_z$ in terms of the scalar amplitudes f_i:

$$\mathcal{A}_x\mathcal{N}_0=\sin\vartheta\,\mathrm{Re}[-f_1f_3^*+f_2f_4^*+\cos\vartheta(-f_1f_4^*+f_2f_3^*)], \tag{6}$$

$$\mathcal{A}_z\mathcal{N}_0=\mathrm{Re}[|f_1|^2+|f_2|^2-2\cos\vartheta f_1f_2^*+\sin^2\vartheta(f_1f_4^*+f_2f_3^*)]. \tag{7}$$

Note that $\mathcal{A}_x$ vanishes at $\vartheta=0^0$ and $\vartheta=\pi$. Moreover, $\mathcal{A}_z=1$ for $\vartheta=0^0$ and $\vartheta=\pi$ for any photon energy. This is a model-independent result, which follows from the conservation of helicity in collinear kinematics. It is correct for any dynamics of the process; its physical meaning is that the collision of γ and p with parallel spins cannot take place for the collinear regime (Fig. 1). This result holds for any process of pseudoscalar and scalar meson photoproduction on a nucleon target (if the final baryon has spin 1/2). Such independence of the P parity of produced mesons is important.

For $\vartheta\neq0$ and $\vartheta\neq\pi$ the results for $\mathcal{A}_x$ and $\mathcal{A}_z$ are model dependent. The models of photon-gluon fusion predict a value for the $\mathcal{A}_z$ asymmetry for the inclusive $\vec{\gamma}+\vec{p}\to\overline{D_c^0}+X$ process $\leqslant30\%$, at $E_\gamma\simeq50$ GeV, depending on the assumptions on the polarized gluon distribution $\Delta G(x)$. Therefore, even a 10% contribution of the exclusive process $\vec{\gamma}+\vec{p}\to\Lambda_c^++\overline{D_c^0}$ to the inclusive $\overline{D_c}$ cross section can induce a large correction to the photon-gluon fusion asymmetry, at forward angles. This should be taken into account in the extraction of ΔG from the asymmetry in the process $\vec{\gamma}+\vec{p}\to\overline{D_c^0}+X$. Evidently the processes considered here, $\gamma+p\to Y_c+\overline{D_c^0}$, do not contribute to the D_c^0 production in the inclusive reaction $\vec{\gamma}+\vec{N}\to D_c^0+X$.

D. Λ_c polarization in $\vec{\gamma}+N\to\vec{\Lambda}_c+\overline{D}_c$

In a similar way it is possible to analyze the polarization properties of the final Λ_c^+ hyperon induced by the initial circular polarization of the photon. Again, due to the P invariance of the electromagnetic hadron interaction, only the $\mathcal{P}_x$ and $\mathcal{P}_z$ components do not vanish. In terms of the scalar amplitudes f_i, defined above, the components of the Λ_c^+ polarization can be written as

$$\mathcal{P}_x\mathcal{N}_0=\lambda\sin\vartheta\,\mathrm{Re}[-2f_1f_2^*-f_1f_3^*+\cos\vartheta(2|f_2|^2+f_2f_3^*-f_1f_4^*)+(2\cos^2\vartheta-1)f_2f_4^*],$$

$$\mathcal{P}_z\mathcal{N}_0=\lambda\,\mathrm{Re}[|f_1|^2-(1-2\cos^2\vartheta)|f_2|^2-2\cos\vartheta f_1f_2^*+\sin^2\vartheta(f_1f_4^*-f_2f_3^*-2\cos\vartheta f_2f_4^*)]. \tag{8}$$

Comparing Eqs. (6), (7), and (8) one can see that the observables $\mathcal{A}_x$ and $\mathcal{A}_z$, on one side, and $\mathcal{P}_x$ and $\mathcal{P}_z$, on another side, are independent in the general case of noncollinear kinematics and contain different physical information. Note also that $\mathcal{P}_z=1$, in case of collinear kinematics ($\cos\vartheta=1$), independently of the model chosen to describe the scalar amplitudes f_i. This rigorous result follows from the conservation of the total helicity in $\gamma+p\to\Lambda_c^+(\Sigma_c^+)+\overline{D}_c^0$, which holds in collinear kinematics. It means that only collisions with particles with antiparallel spins in the entrance channel are allowed (see Fig. 1); i.e., the final Λ_c hyperon is polarized along the direction of the spin of the initial photon. This result holds for any $Y_c+\overline{D_c}$ final state independently of the P parity of the $N\Lambda_cD_c$ system.

At $\vartheta=0^0$ or $\vartheta=\pi$, the observable $\mathcal{P}_x$ vanishes. This follows from the axial symmetry of the collinear kinematics, where only one physical direction can be defined (along the z axis). In such kinematical conditions the x and y axes are arbitrary; therefore, $\mathcal{P}_x=\mathcal{A}_x=0$. It is a very general result, also independent of the relative $P(N\Lambda_cD_c)$ parity. Again, in noncollinear kinematics, the behavior of $\mathcal{P}_x$ and $\mathcal{P}_z$ can be predicted only in the framework of a model.

The measurement of the Λ_c^+ polarization can be done similarly to the strange Λ^0 hyperon, because Λ_c^+, being the lightest charm baryon, can decay only through the weak interaction. However, the Λ_c^+ hyperon decays through many channels with different branching ratios and analyzing powers. Let us mention, for example, the two-particle decay $\Lambda_c^+\to\Lambda^0+\pi^+$, which has a large decay asymmetry $A=0.98\pm0.19$, but a relatively small branching ratio $B(\Lambda\pi)=(9.0\pm2.8)\times10^{-3}$. The semileptonic Λ_c^+ decay $\Lambda_c^+\to\Lambda^0+e^++\nu_c$ is characterized by a larger branching ratio $B(\Lambda e\nu)=(2.1\pm0.6)\%$ with relatively large decay asymmetry (in absolute value) $A=-0.82^{+0.11}_{-0.007}$ [35]. Note that the

[2]Note that we consider here only double-spin correlations, neglecting in particular the T-odd analyzing power, induced by the $\mathcal{P}_y$ component of the target polarization.

possibility to measure the Λ_c^+ polarization has been experimentally confirmed in hadronic collisions [36].

It is not the case for the Σ_c hyperon. Its main decay $\Sigma_c \to \Lambda_c + \pi$ is due to the strong interaction. So whereas the Λ_c^+ is a self-analyzing particle, the Σ_c hyperon is similar, in this respect, to any baryon resonance, with strong or electromagnetic decays.

E. Depolarization coefficients

Let us consider for completeness other double-spin polarization observables, the coefficients of polarization transfer $\mathcal{D}_{ab}$, from a polarized proton target to a Λ_c hyperon, which can be defined as

$$\mathcal{N}_0 \mathcal{D}_{ab} = \frac{1}{2} \mathrm{Tr}\ \mathcal{F} \vec{\sigma} \cdot \vec{a} \mathcal{F}^\dagger \vec{\sigma} \cdot \vec{b}.$$

The index a ($a=m,n,k$) refers to the component of the proton polarization, whereas the index b ($b=m,n,k$) refers to the component of the Λ_c polarization. The unit vectors $\hat{\vec{m}}$, $\hat{\vec{n}}$, and $\hat{\vec{k}}$ are defined as follows: $\hat{\vec{k}} = \vec{k}/|\vec{k}|$, $\hat{\vec{n}} = \vec{k} \times \vec{q}/|\vec{k} \times \vec{q}|$, $\hat{\vec{m}} = \hat{\vec{n}} \times \hat{\vec{k}}$.

Only five among these coefficients are nonzero (for unpolarized photons):

$$\begin{aligned}
\mathcal{N}_0 \mathcal{D}_{mm} &= \frac{\sin^2\vartheta}{2} \mathrm{Re}[(2\sin^2\vartheta - 1)|f_4|^2 - |f_3|^2 + 2 + f_1 f_4^* \\
&\quad - 2 f_2 f_3^* - 2\cos\vartheta (2 f_2 f_4^* - f_3 f_4^*)], \\
\mathcal{N}_0 \mathcal{D}_{nn} &= -\frac{\sin^2\vartheta}{2} \mathrm{Re}[|f_3|^2 + |f_4|^2 \\
&\quad + 2(f_1 f_4^* + f_2 f_3^* + \cos\vartheta f_3 f_4^*)], \\
\mathcal{N}_0 \mathcal{D}_{kk} &= -\mathrm{Re}\Big\{ |f_1|^2 + (1 - 2\cos^2\vartheta)|f_2|^2 + 2\cos\vartheta f_1 f_2^* \\
&\quad + \frac{\sin^2\vartheta}{2} [|f_3|^2 + (2\cos^2\vartheta - 1)|f_4|^2 \\
&\quad + 2(f_2 f_3^* - f_1 f_4^* + \cos\vartheta (2 f_2 f_4^* + f_3 f_4^*)] \Big\}, \\
\mathcal{N}_0 \mathcal{D}_{mk} &= \sin\vartheta\, \mathrm{Re}[\sin^2\vartheta (\cos\vartheta |f_4|^2 + f_3 f_4^*) + 2 f_1 f_2^* \\
&\quad + f_1 f_3^* + (1 - 2\cos^2\vartheta) f_2 f_4^* \\
&\quad + \cos\vartheta (-2|f_2|^2 + f_1 f_4^* - f_2 f_3^*], \\
\mathcal{N}_0 \mathcal{D}_{km} &= \sin\vartheta\, \mathrm{Re}[\sin^2\vartheta (\cos\vartheta |f_4|^2 + f_3 f_4^*) \\
&\quad + \cos\vartheta (f_1 f_4^* - f_2 f_3^*) + f_1 f_3^* \\
&\quad + (1 - 2\cos^2\vartheta) f_2 f_4^*]. \qquad (9)
\end{aligned}$$

Note that $\mathcal{D}_{km} \neq \mathcal{D}_{mk}$, because the process $\gamma + N \to Y_c + \bar{D}_c$ is asymmetrical with respect to initial and final baryons, so these coefficients contain different information about the amplitudes f_i and therefore about the reaction mechanisms.

Comparing Eqs. (4) and (9) one can see that $\Sigma_B = \mathcal{D}_{nn}$. This relation is valid in the general case for any kinematical condition and any choice of reaction mechanism. In the case of positive relative P parity of the D_c meson with respect to the $N\Lambda_c$ system, $P(N\Lambda_c D_c) = +1$, we find, instead, $\Sigma_B = -\mathcal{D}_{nn}$. Therefore we can write $\Sigma_B = -P(N\Lambda_c D_c)\mathcal{D}_{nn}$ and suggest another possible and model-independent method to measure $P(N\Lambda_c D_c)$ through a test of the relative sign of these two observables.

III. DISCUSSION OF THE REACTION MECHANISMS

The charm particle photoproduction and electroproduction at high energy is usually interpreted in terms of photon-gluon fusion, $\gamma + G \to c + \bar{c}$ [Fig. 2(a)]. Near threshold, another possible mechanism, based on the subprocess $q + \bar{q} \to G \to c + \bar{c}$ [Fig. 2(b)], should also be taken into account, as was done for πN collisions [37]. In the case of the exclusive reactions $\gamma + N \to Y_c + \bar{D}_c$ ($\bar{D}_c^*$), $Y_c = \Lambda_c, \Sigma_c$, the mechanism in Fig. 2(b) is equivalent to the exchange of a $\bar{c}q$ system, in the t channel [Fig. 2(c)]. The importance of the annihilation mechanism has been investigated in [38] to explain the forward charge asymmetry in γp collisions. The mesonic equivalent of such exchange is the exchange by pseudoscalar $\bar{D}_c$ and (or) vector $\bar{D}_c^*$ mesons, in the t channel of the considered reaction.

To move further, one has to take into account the symmetry property of electromagnetic hadronic interactions, such as conservation of the electromagnetic current. This makes the principal difference between γN and πN production of charmed particles. If in the case of D_c^* exchange in $\gamma + N \to Y_c + \bar{D}_c$ the corresponding matrix element is gauge invariant, for any kinematical conditions and any values of the coupling constants, as a result of the magnetic dipole transition in the vertex $D_c^* \to D_c + \gamma$, it is not the case for the pseudoscalar D_c^- exchange in the reaction $\gamma + p \to \Sigma_c^{++} + D^-$, for example. The D_c^- exchange alone cannot satisfy the gauge invariance; therefore, other mechanisms have to be added, such as baryonic exchanges in s and u channels (Fig. 3).

Note that only the sum of s, t, and u exchanges gives a gauge-invariant total matrix element for $\gamma + N \to Y_c + \bar{D}_c$. More exactly this holds for pseudoscalar interactions in the vertex $N \to Y_c + \bar{D}_c$. In case of the pseudovector vertex, which can also be considered, gauge invariance is ensured by an additional contribution of the so-called ''catastrophic'' (contact) diagram (Fig. 4), which has a definite spin structure and a known coupling constant $g_{NY_c\bar{D}_c}$.[3]

Following the equivalence theorem, both these ap-

[3]Note, in this respect, that direct estimation of this contact contribution to the cross section of the process $\gamma + p \to \Sigma_c^{++} + D_c^-$ [39] results in a too large cross section in the near-threshold region, in contradiction with the experimental data [40].

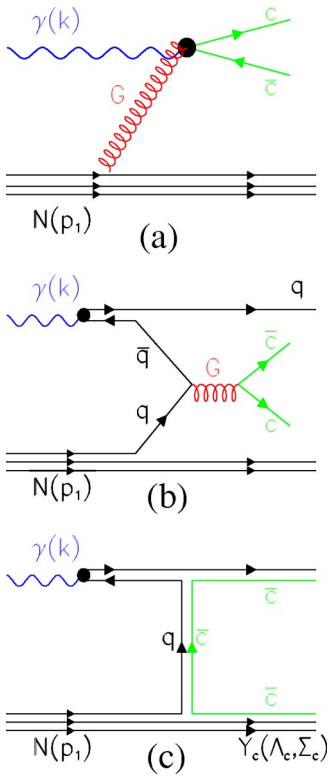

FIG. 2. Feynman diagrams for associative charm production in γN collisions: (a) the subprocess of photon-gluon fusion, $\gamma+G\to c+\bar{c}$; (b) the subprocess of $q+\bar{q}$ annihilation, $q+\bar{q}\to c+\bar{c}$; (c) t-channel exchange by $\bar{D}_c$ and $\bar{D}_c^*$ for $\gamma+N\to Y_c+\bar{D}_c(\bar{D}_c^*)$.

proaches result in the same matrix element for the "electric" interaction, induced by the electric charges of the participating hadrons. But the magnetic moments of the nucleons and the Y_c hyperons produce different results for pseudoscalar and pseudovector interactions, showing the relevance of off-mass-shell effects in the considered model.

Of course, the magnetic moments of baryons cannot violate the gauge invariance for any numerical value and in any kinematical condition.

To take into account the virtuality of the exchanged hadrons, in this approach, form factors (FFs) are introduced in the pole diagrams. For baryonic exchange the corresponding FFs can be parametrized as [41]

$$F_N(s)=\frac{\Lambda_N^4}{\Lambda_N^4+(s-m^2)^2},\quad F_Y(u)=\frac{\Lambda_Y^4}{\Lambda_Y^4+(u-M^2)^2},\tag{10}$$

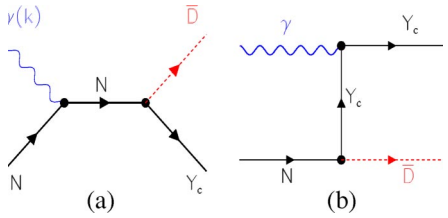

FIG. 3. Baryon exchanges in the s channel (a) and u channel (b) for the process $\gamma+N\to Y_c+\bar{D}_c$.

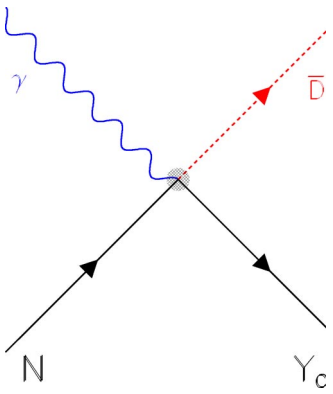

FIG. 4. The catastrophic diagram for $\gamma+N\to\bar{D}_c+Y_c$ for the pseudovector $NY_c\bar{D}_c$ interaction.

where Λ_N and Λ_Y are the corresponding cutoff parameters, $s=(k+p_1)^2$, $u=(k-p_2)^2$, k, p_1, and p_2 are the four-momenta of the photon, the nucleon, and the hyperon, respectively, and m (M) is the nucleon (hyperon) mass.

For mesonic exchanges, another expression of FFs is taken:

$$F_D(t)=\frac{\Lambda_{1\gamma}^2-m_D^2}{\Lambda_{1\gamma}^2-t}\,\frac{\Lambda_1^2-m_D^2}{\Lambda_1^2-t},$$

$$F_{D*}(t)=\frac{\Lambda_{2\gamma}^2-m_{D*}^2}{\Lambda_{2\gamma}^2-t}\,\frac{\Lambda_2^2-m_{D*}^2}{\Lambda_2^2-t},\tag{11}$$

where $t=(k-q)^2=(p_1-p_2)^2$, m_D (m_D^*) is the mass of the D (D^*) meson, $\Lambda_{1,2\gamma}$ are the cutoff parameters for the electromagnetic vertex, $\gamma+D_V(D_V^*)\to D$, with virtual $D(D^*)$ mesons, and $\Lambda_{1,2}$ are the cutoff parameters for the strong vertex $N\to Y_c+D_V(D_V^*)$. All these FFs are normalized such that $F_N(s=m^2)=F_Y(u=M^2)=F_D(t=m_D^2)=F_{D*}(t=m_{D*}^2)=1$.

Only for the magnetic contributions do these expressions of FFs not destroy the gauge invariance of the total matrix element. Once these FFs, which are different for different diagrams, are introduced, the other contributions, induced by the electric charges of the particles, will be rearranged in such a way that the gauge invariance is strongly violated. The simplest way to restore the gauge invariance is to multiply the complete matrix element (for $s+t+u$ contributions) by a common factor [41]:

$$\frac{1}{3}[F_N(s)+F_Y(u)+F_D(t)],\quad \text{for}\quad \gamma+N\to Y_c+D_c^-,$$

$$\frac{1}{2}[F_N(s)+F_Y(u)],\qquad \text{for}\quad \gamma+N\to Y_c+\bar{D}_c^0.$$

Such a term is a function of both independent kinematical variables; therefore, it cannot be rigorously called a form factor, which must be, in general, a function of one variable only.

These terms decrease essentially the differential cross sections at large values of $|t|$ or $|u|$ and, therefore, the total cross section, especially in the near-threshold region. The role of FFs is essential for such an approach, as has been proved in the analysis of vector meson or strange particle production in NN and ΔN collisions [42]. Particularly large effects appear for the processes of open charm production in exclusive reactions, such as $N+N\to Y_c+\bar{D}_c+N$ [43,44]. But polarization phenomena are, in principle, less sensitive to FFs. Moreover, in the limiting case of $s+u+t(D_c)$ contributions (without D_c^*) or only vector D_c^* exchange, one can see that polarization observables are independent of any phenomenological FFs, for any kinematics. Such models can generate only T-even polarization observables, such as Σ_B asymmetry, induced by linearly polarized photons, or $A_{x,z}$ asymmetries, induced by the collision of circularly polarized photons with a polarized proton target.

Summarizing this discussion, one can note that application of the ELA to exclusive charm meson photoproduction is based on an analogy with standard calculations on light mesons (pions, kaons, . . .). In this respect, one can note an approximative scaling of the masses of the exchanged mesons, $m_K/m_\pi \simeq m_D/m_K$, which are important quantities of the model. But in the case of charm meson exchanges, t-channel poles occur far from the physical region of kinematical variables, and the model cannot be justified by this kind of arguments. The basis of the ELA model is a definite set of pole diagrams (in s, t, and u channels) with effective coupling constants and phenomenological form factors. The t exchange give poles located nearer to the physical region, in comparison with s and u channels. The choice of an adequate mechanism for $\gamma+N\to Y_c+\bar{D}_c$ is dictated by the gauge invariance of the electromagnetic interaction and the SU(4) symmetry (which can be violated). In the absence of other theoretical approaches, the ELA appears as a powerful tool for the predictions of the physical observables, as long as the number of unknown parameters is limited or can be estimated from other sources.

IV. MATRIX ELEMENTS FOR $\gamma+N\to Y_C+\bar{D}_C$, $Y_c=\Lambda_c,\Sigma_c$

Let us consider in detail the matrix elements for the reactions of $\gamma+N\to Y_c+\bar{D}_c$, $Y_c=\Lambda_c,\Sigma_c$, considering s, u, and $t(\bar{D}_c+\bar{D}_c^*)$ contributions:

$$\mathcal{M}=\mathcal{M}_s+\mathcal{M}_u+\mathcal{M}_t(D)+\mathcal{M}_t(D^*).$$

For the pseudoscalar $N\bar{D}_cY_c$ vertex, the matrix element for one-nucleon exchange in the s channel, $\mathcal{M}_s$, can be written as follows:

$$\mathcal{M}_s=\frac{eg_{NY_cD}}{s-m^2}\bar{u}(p_2)\gamma_5(\hat{p_1}+\hat{k}+m)\left(Q_N\hat{\epsilon}-\kappa_N\frac{\hat{\epsilon}\hat{k}}{2m}\right)u(p_1), \tag{12}$$

where κ_N is the anomalous magnetic moment of the nucleon, g_{NY_cD} is the coupling constant for the vertex $N\to Y_c+D_c$, and Q_N is the electric charge of the nucleon. We assume, in Eq. (12) (and later on in this paper), that the relative P parity of the $N\bar{D}_cY_c$ system is negative, in agreement with the quark model. In principle, this P parity can be experimentally determined [45].

The other matrix elements can be written as

$$\mathcal{M}_u=\frac{eg_{NY_cD_c}}{u-m^2}\bar{u}(p_2)\left(Q_{Y_c}\hat{\epsilon}-\kappa_{Y_c}\frac{\hat{\epsilon}\hat{k}}{2M}\right)\times(\hat{p_2}-\hat{k}+M)\gamma_5u(p_1), \tag{13}$$

$$\mathcal{M}_t(D_c)=\frac{eg_{NY_cD}}{t-m_D^2}Q_D\bar{u}(p_2)\gamma_5u(p_1)2\epsilon\cdot q,$$

$$\mathcal{M}_t(D_c^*)=i\frac{eg_{NY_cD^*}}{t-m_{D^*}^2}\frac{g_{D^*D\gamma}}{m_{D^*}}\epsilon_{\mu\nu\alpha\beta}\epsilon_\mu k_\nu\mathcal{J}_\alpha(k-q)_\beta, \tag{14}$$

where Q_{Y_c} and $Q_{\bar{D}_c}$ are the electric charges of the Y_c hyperon and of the $\bar{D}_c$ meson, so that $Q_N=Q_{Y_c}+Q_{\bar{D}_c}$, ϵ_ν is the four-vector of photon polarization, and $\mathcal{J}_\alpha$ is the vector current for the vertex $N\to Y_c+D_c^*$:

$$\mathcal{J}_\alpha=\bar{u}(p_2)\left[\gamma_\alpha(1+\kappa_{Y_c})-\kappa_{Y_c}\frac{p_{1\alpha}+p_{2\alpha}}{m+M}\right]u(p_1), \tag{15}$$

where $g_{NY_cD^*}$ and $\kappa_{Y_c}g_{NY_cD^*}$ are the vector (Dirac) and the tensor (Pauli) coupling constants for the vertex $D_c^*N\to Y_c$ and $g_{D^*D\gamma}$ is the coupling constant for the vertex $D_c^*\to D_c\gamma$. The corresponding width $\Gamma(D_c^*\to D_c\gamma)$ in terms of $g_{D^*D\gamma}$ can be written as follows:

$$\Gamma(D_c^*\to D_c\gamma)=\frac{\alpha}{24}m_{D^*}\left(1-\frac{m_D^2}{m_{D^*}^2}\right)^3g_{D^*D\gamma}^2,$$

$$\alpha=\frac{e^2}{4\pi}\simeq\frac{1}{137}.$$

From the experimental data about D_c^{*+} decays [35],

$$\Gamma(D_c^{*+})=(96\pm4\pm22)\ \text{keV},$$

$$\mathrm{Br}(D_c^*\to D_c\gamma)=(1.68\pm0.42\pm0.49)\%,$$

one can find $|g_{D^{*+}D^+\gamma}|=1.03$. The sign of this constant cannot be determined from these data. The situation with the coupling $g_{D^{*0}D^0\gamma}$ is less definite. Having the largest branching ratio $\mathrm{Br}(D_c^{*0}\to D_c^0\gamma)\simeq40\%$, only the upper limit is experimentally known for the total width of neutral D^{*0}: $\Gamma(D_c^{*0})\leqslant2.1$ MeV [35]: i.e., $\Gamma(D_c^{*0}\to D_c^0\gamma)\leqslant840$ keV—i.e., very far from the theoretical predictions [46], with $\Gamma(D_c^{*0}\to D_c^0\gamma)\geqslant10$ keV.

The expressions for the scalar amplitudes f_i, corresponding to the different matrix elements, Eqs. (12)–(15), are given in the Appendix.

V. DISCUSSION OF THE RESULTS

The main ingredients of the considered model, which enter in the numerical calculations of the different observables for the exclusive process $\gamma+N\to Y_c+\bar{D}_c$, are the strong and electromagnetic coupling constants and the phenomenological FFs.

A. Electromagnetic coupling constants

The electromagnetic characteristics of the charmed particles, such as the magnetic moments of the Y_c hyperon and the $g_{D^*D\gamma}$ coupling constants (transition magnetic moments), are not well known. Only the width of the radiative decay $D_c^{*+}\to D_c^+ + \gamma$ has been directly measured, which allows one to derive the corresponding coupling constant $g_{D^{*+}D^+\gamma}$ but not its sign. The magnetic moments of the charmed hyperons and the transition magnetic moment $g_{D^{*0}D^0\gamma}$ are not experimentally known.

Based on previous experience with the theoretical description of the magnetic moments of strange hyperons and of the transition magnetic moments of the decays $V\to P+\gamma$ (with vector $V=\rho$, ω, ϕ, K^* and pseudoscalar $P=\pi$, η, K light mesons), one can assume that predictions from symmetry considerations may work in this region of hadron electromagnetic interactions.

We will use different theoretical approaches to extrapolate these quantities to charm particle electrodynamics, in particular to the magnetic moments of Y_c and to the amplitude of the radiative decay $D_c^*\to D_c+\gamma$. Quark models, SU(4) symmetry, QCD dispersion sum rules, and effective chiral theories with heavy quarks can also give useful guidelines.

The dependence of some observables for the reactions $\gamma+N\to Y_c+\bar{D}_c$ on the magnetic moments of the charmed baryons has been studied in [9]. Here, for all the calculations, we take the $\mu\Lambda_c^+$ value from [47], but for the Σ_c hyperons we take the U(4) predictions [8]:

$$\mu(\Sigma_c^{++})=\frac{2}{3}\mu_p,\quad \mu(\Sigma_c^{+})=0,\quad \mu(\Sigma_c^{0})=-\frac{2}{3}\mu_p.$$

B. Strong-coupling constants

We call strong-coupling constants those which involve one nucleonic vertex: $g_{NY_c\bar{D}_c}$, $g_{NY_c\bar{D}_c^*}$, and κ_{Y_c}, $Y_c=\Lambda_c$, or Σ_c. Six coupling constants enter in the calculation of the different observables (three for $\gamma+N\to\Lambda_c+\bar{D}_c$ and three for $\gamma+N\to\Sigma_c+\bar{D}_c$) and of their E_γ and $\cos\vartheta$ dependences, for all the possible exclusive reactions of associative charm particle photoproduction, $\gamma+N\to Y_c+\bar{D}_c$.

Note that the same coupling constants enter in the description of charmed particle production in πN collisions $\pi+N\to Y_c+\bar{D}_c$, NN collisions $N+N\to N+Y_c+\bar{D}_c$, and in the interaction of charmed particles with nuclei in heavy ion collisions, $D_c+N\to Y_c+P(V)$, $Y_c+N\to N+N+D_c$, etc.

The lack of experimental data about these processes does not allow one to fix these coupling constants. Therefore the typical way to estimate these couplings is to rely on SU(4) symmetry and connect the necessary coupling constants with the corresponding constants for strange particle production:

$$g_{N\Lambda(\Sigma)K},\quad g_{N\Lambda(\Sigma)K^*},\quad \kappa_{N\Lambda(\Sigma)K^*}, \tag{16}$$

taking into account that the strange quark is the heaviest of the three light quarks (u,d,s), and the charmed quark is the lightest of the three heavy quarks (c,b,t).

The coupling constants (16) for strange particles have been estimated from several experiments in photoproduction and electroproduction of strange particle on nucleons, $\gamma+N\to\Lambda(\Sigma)+K$ and $e^-+N\to e^-+\Lambda(\Sigma)+K$ [48]. However, different models predict different sets of constants (16), which can take values in a wide interval.

This gives, nevertheless, a starting point of our analysis, applying SU(4) symmetry. We have also to keep in mind that SU(4) symmetry can be strongly violated, at least at the scale of the difference in the masses of charmed and strange particles (induced by the difference in the masses of c and s quarks).

C. Phenomenological form factors

In order to determine the form factors, one has to choose a convenient analytical parametrization and then numerical values for the cutoff parameters Λ_N, $\Lambda_{1,2}$, and $\Lambda_{1,2\gamma}$. Generally one takes a monopole, dipole, or exponential dependence on the momentum transfer. One possibility is to choose as argument of these FFs the four-momentum transfer squared, but one can also take the three-momentum transfer, as well. In this last case, the corresponding reference frame has to be indicated.

The numerical values of the cutoff parameters can be determined from the previous experience in the interpretation of other photoproduction and hadroproduction processes, in the framework of the ELA approach. In the present calculations we use the parametrizations for the corresponding FFs, following Eqs. (10) and (11).

D. Three possible scenarios

Summarizing the previous discussion, one can conclude that SU(4) symmetry gives some guidelines to fix the necessary parameters of the calculation (strong-coupling constants and Y_c magnetic moments). Note that not only the absolute values of these couplings are important in our considerations, but also their relative signs, due to the strong interference effects between the different contributions. The relative signs of s, u, and $t(D)$ contributions to the matrix element of any exclusive process $\gamma+N\to Y_c+\bar{D}_c$ are uniquely fixed by the requirement of gauge invariance. But it is not the case for the relative sign of the D^* contribution, so one must make some assumptions, such as the validity of SU(6) symmetry. It is important to stress that such a symmetry consideration is reliable for the prediction of relative signs, but not for the absolute values of the considered couplings.

Any fitting procedure induces a strong correlation between the cutoff parameters and the strong-coupling constants. Therefore there is no unique solution, and we will consider three possible scenarios.

(i) The strong-coupling constants are fixed by SU(4) symmetry, using the corresponding values for the strange coupling constants (16), found in the analysis of experimental data [48] on associative strange particles photoproduction and electroproduction. Only the cutoff parameters are fixed on the charm photoproduction data. We assume, for simplicity,

$$\Lambda_1=\Lambda_2=\Lambda_{1\gamma}=\Lambda_{2\gamma}\equiv\Lambda, \quad \Lambda_Y=\Lambda_N.$$

(ii) We assume that SU(4) symmetry is strongly violated for the strong-coupling constants. So we take for the couplings (16) some arbitrary values, far from SU(4) predictions, and both cutoff parameters Λ and Λ_N are determined from charm photoproduction data.

(iii) We assume that SU(4) symmetry is violated only for the $N\to\Lambda_c+\bar{D}_c^*$ vertex, but for the couplings g_1 and g_2 we take the SU(6) values of the corresponding coupling constants for the vertex $N\to\Lambda+K^*$. Again the parameters Λ_N and Λ are fixed from charm photoproduction data at $E_\gamma=20$ GeV.

Taking into account the limited experimental data about charm particle photoproduction, one cannot do a rigorous fit for all the parameters of the model.

The model can predict the energy behavior of the total cross section for $\gamma^*+N\to Y_c+D_c$ (for proton and neutron targets), for each of the three versions. Therefore we normalize the total cross section for $\gamma+p\to\Lambda_c^++\bar{D}_c^0$, which is the largest from all the exclusive reactions $\gamma+p\to Y_c+\bar{D}_c$, to the measured cross section of open charm photoproduction at $E_\gamma=20$ GeV [3], where it was found that about 70% of the total cross section can be attributed to $\gamma+p\to\Lambda_c^++\bar{D}_c^0$. This condition constrains very strongly the parameters for all three versions of the model, as this reaction has the largest cross section.

The parameters are reported in Table I. We use the following notation: $g_1=g_{N\Lambda_cD^*}$, $g_2=g_{N\Lambda_cD^*}$.

Our procedure is not a real fit, as we take into account only the low-energy point; therefore, we do not give any χ^2 estimates of the quality of the model in its three versions.

Once the parameters have been fixed, Table I, one can predict all polarization observables not only for $\gamma+p\to\Lambda_c^++\bar{D}_c^0$ but also for any exclusive reaction $\gamma+N\to Y_c^++\bar{D}_c$. For the reactions with Σ_c production, we take the following coupling constants: $g_{N\Sigma_c\bar{D}_c}=4.5$, $g_1(N\Sigma_c\bar{D}_c^*)=-g_2(N\Sigma_c\bar{D}_c^*)=-25$, which correspond to the values of $g_{N\Sigma K}$ and $g_{N\Sigma K^*}$, obtained from a fit to the experimental data about $\gamma+p\to\Lambda(\Sigma^0)+K^+$ and $e+p\to e+\Lambda(\Sigma^0)+K^+$ [48]. For the cutoff parameters we took the values $\Lambda_N=0.8$ and $\Lambda=2.4$ GeV, as for model I.

The energy dependence of the total cross section for the six exclusive processes $\gamma+N\to Y_c+\bar{D}_c$ is very different in the entire photon energy range, Fig. 5. For $E_\gamma\geqslant 40$ GeV, the predicted energy dependence of the total cross section becomes flat, up to $E_\gamma=250$ GeV. One can conclude that, in this energy range, the simplest exclusive photoproduction reactions $\gamma+N\to Y_c^++\bar{D}_c$ contribute less than 10% to the total cross section of open charm photoproduction. This estimation does not contradict the existing experimental data and is in agreement with the measured Λ/Λ_c asymmetry (in sign and value).

TABLE I. Parameters for models I, II, III; see text. The cutoff parameters Λ_N and Λ are expressed in GeV.

Model	$g_{N\Lambda_cD}$	g_1	g_2	Λ_N	Λ
I	-11.5	-23	-57.5	0.8	2.4
II	$-2.$	-2.5	$-6.$	1.6	3.4
III	$-2.$	$-6.$	$-22.$	0.6	2.7

It is interesting to note that we have very large isotopic effects—i.e., a large difference in the absolute values and behavior for the different channels with different charges of the participating hadrons. This is an expected property of the ELA, because the relative values of *s*-, *u*-, and *t*-channel contributions are different for the different channels. Note that the largest cross section on the neutron target belongs to the process $\gamma+n\to\Sigma_c^0+\bar{D}^0$, the D^- production being essentially suppressed. Moreover, the D^- production is also small in the γp interaction $\gamma+p\to\Sigma_c^{++}+D^-$, in agreement with the experiment [4]. The total cross section as a function of the photon energy, for the reaction $\gamma+p\to\Lambda_c^++\bar{D}^0$, is shown in Fig. 6 for the three sets of parameters. After a fast increase near threshold, the cross section is quite flat for

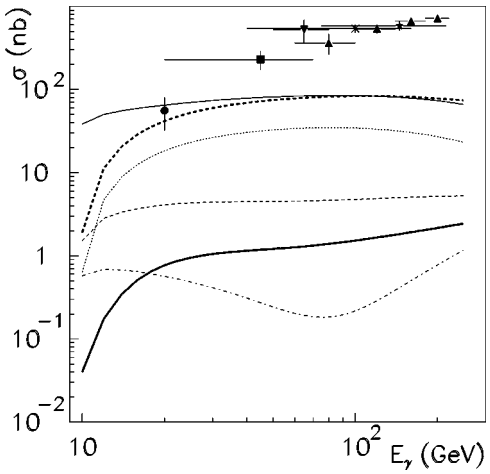

FIG. 5. E_γ dependence of the total cross section for the photoproduction of charmed particles for model I. The curves correspond to different reactions $\gamma+p\to\Lambda_c^++\bar{D}^0$ (solid line), $\gamma+p\to\Sigma_c^{++}+D^-$ (dashed line), $\gamma+p\to\Sigma_c^++\bar{D}^0$ (dotted line), $\gamma+n\to\Lambda_c^++D^-$ (dot-dashed line), $\gamma+n\to\Sigma_c^++D^-$ (thick solid line), $\gamma+n\to\Sigma_c^0+\bar{D}^0$ (thick dashed line). The data correspond to the total charm photoproduction cross section from [1] (reverse triangle), [4] (square), [6] (asterisk), [5] (star), [2] (triangles), [3] (circle).

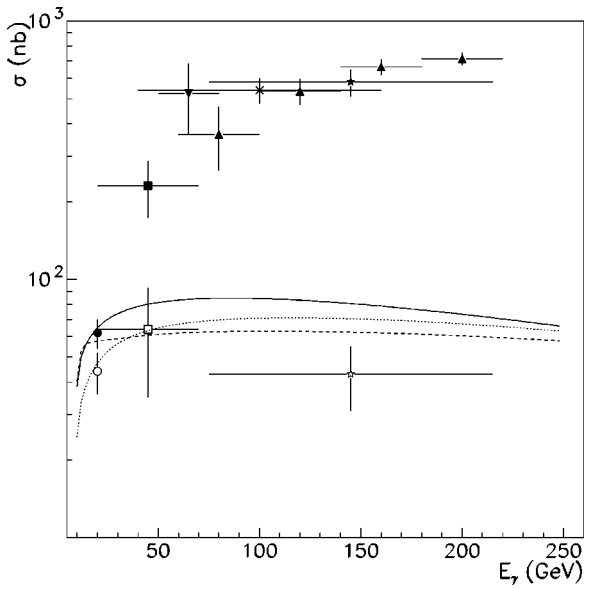

FIG. 6. E_γ-dependence of the total cross section for the reaction $\gamma+p\to\Lambda_c^+ + \bar{D}_c^0$ for model I (solid line), II (dashed line) and III (dotted line). Solid symbols as in Fig. 5, open symbols are from [3] (open circle), from [4] (open square), and from [5] (open star).

$E_\gamma > 50$ GeV and represents about 10% of the total cross section. Estimations of associative charm photoproduction cross sections, which have been done from experiments [3–5], are reported as open symbols in Fig. 6.

E. Contribution to $\bar{D}_c/D_c$ asymmetries

Our aim here is to have a realistic view of the general characteristics of the different reaction channels, for charm photoproduction, in a region which is accessible by experiments. A large antiparticle/particle asymmetry, not explainable in terms of perturbative QCD (PQCD) models, has been reported in the literature.

The observation of the $\bar{D}_c^0/D_c^0$ or $\bar{\Lambda}_c/\Lambda_c$ asymmetry in γN collisions is important in order to test the validity of the photon-gluon fusion mechanism. The discussed asymmetries are defined as

$$A=\frac{N(\bar{c})-N(c)}{N(\bar{c})+N(c)},$$

where $N(c)$ $[N(\bar{c})]$ is the number of corresponding charm particles (D or Λ_c) containing $c[\bar{c}]$ quarks.

Note that the exclusive photoproduction of open charm in the processes $\gamma+N\to Y_c+\bar{D}_c\ \bar{D}_c^*$ will result in $\bar{D}^0/D^0$ and $\bar{\Lambda}_c/\Lambda_c$ asymmetry in γN collisions (with unpolarized particles), increasing the $\bar{D}_c$ production and decreasing the $\bar{\Lambda}_c$ production. Such asymmetries have been experimentally observed [49]. For example, the FOCUS experiment found an asymmetry for $\bar{\Lambda}_c/\Lambda_c$ production of $\simeq -(0.14\pm 0.02)$ at $E_\gamma \simeq 180$ GeV, demonstrating that Λ_c^+ production is more probable than $\bar{\Lambda}_c$ [50]. At similar energies the E687 experiment finds enhancement of $\bar{D}_c$ over D_c production [51]. Very large (in absolute value) charm asymmetries have been observed also at $E_\gamma = 20$ GeV at SLAC [3]. Note also that the SELEX Collaboration presented results on the $\bar{\Lambda}_c/\Lambda_c$ asymmetries for different hadronic processes p, π^-, $\Sigma^- + N\to \Lambda_c^\pm + X$ [52]. Similar results have been presented by the Fermilab E791 Collaboration [53]. This is in contradiction with the model of photon-gluon fusion, which predicts symmetric $\bar{\Lambda}_c$-Λ_c yields and can be considered as an indication of the presence of other mechanisms. The exclusive processes $\gamma + N\to Y_c + \bar{D}_c$ discussed in this paper explain naturally such a asymmetry.

F. Differential cross section and polarization observables

The prediction of the $\cos\vartheta$ dependence of $(d\sigma/d\Omega)_0$, Σ_B, $\mathcal{A}_x$, $\mathcal{A}_z$, $\mathcal{P}_x$, and $\mathcal{P}_z$, for the six processes $\gamma+N\to Y_c + \bar{D}_c$ ($Y_c=\Lambda_c^+$, Σ_c) on proton and neutron targets is shown in Figs. 7 and 8, for model I, at $E_\gamma = 15$ GeV.

Note that, for any version of the considered model, the asymmetry Σ_B is positive in the whole angular region, in contradiction with the predictions of PGF [10] and in agreement with the SLAC data [3].

At the same energy, for the same reactions, with similar notation, the depolarization coefficients $\mathcal{D}_{ab}$ are shown in Figs. 9 and 10.

Polarization effects are generally large (in absolute value), characterized by a strong $\cos\vartheta$ dependence, which results from a coherent effect of all the considered pole contributions. Large isotopic effects (i.e., the dependence on the electric charges of the participating hadrons) are especially visible in the $\cos\vartheta$ distributions for all these observables.

The dependence of these observables on the version of the model, at $E_\gamma = 15$ GeV, for the reaction $\gamma+p\to\Lambda_c^+ + \bar{D}^0$ is shown in Fig. 11. For the same reaction, the $\cos\vartheta$ dependence of the individual s, u, and $t(D^*)$ contributions to the differential cross section and to the considered polarization observables is shown in Fig. 12. This behavior is the same for any version of the considered model, the difference appearing in the interference of the various contributions.

Figure 13 shows, for model I, the energy dependence of the integrated $\bar{\mathcal{A}}_z(E_\gamma)$ asymmetry, for $\vec{\gamma}+\vec{p}\to\Lambda_c^+ + \bar{D}^0$, which is defined as

$$\bar{\mathcal{A}}_z(E_\gamma)=\frac{\int_{-1}^{+1}\mathcal{N}_0\mathcal{A}_z(E_\gamma,\cos\vartheta)\,d\cos\vartheta}{\int_{-1}^{+1}\mathcal{N}_0\,d\cos\vartheta}.$$

This asymmetry is large near threshold, taking its maximum value $\mathcal{A}_z=+1$ at threshold. It decreases with energy, due to the fact that the cross section increases with energy and then flattens, whereas the $t(D^*)$ contribution becomes more important. The interference of the $t(D^*)$ channel with s and u channels essentially decreases the $\mathcal{A}_z(E_\gamma)$ asymmetry, outside collinear kinematics, where $\mathcal{A}_z(E_\gamma)=+1$ for all contributions.

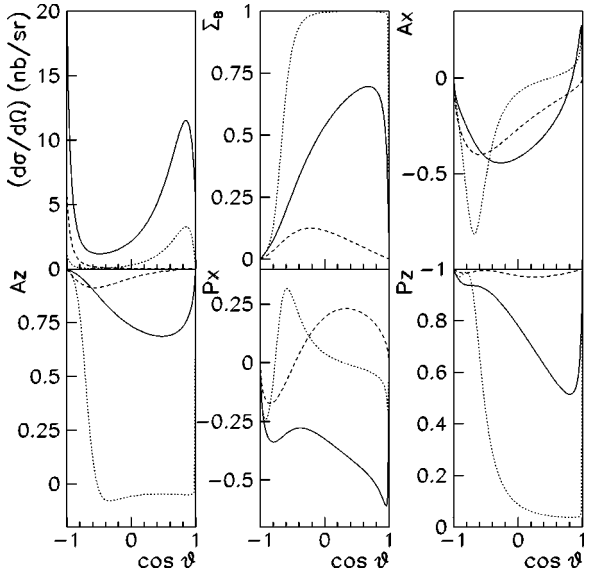

FIG. 7. Differential cross section and polarization observables Σ_B, $\mathcal{A}_x$, $\mathcal{A}_z$, $\mathcal{P}_x$, and $\mathcal{P}_z$, for the reactions $\gamma+p\to\Lambda_c^+ +\overline{D}_c^0$ (solid line), $\gamma+p\to\Sigma_c^{++}+D_c^-$ (dashed line), and $\gamma+p\to\Sigma_c^+ +\overline{D}_c^0$ (dotted line), calculated for model I.

For comparison, predictions for this observable in inclusive charm photoproduction are also shown. These predictions have been done in the framework of the standard QCD approach, assuming the PGF model (Fig. 2), calculating the ratio of the elementary cross sections for $\gamma+G\to c+\overline{c}$ folded with the gluon distributions:

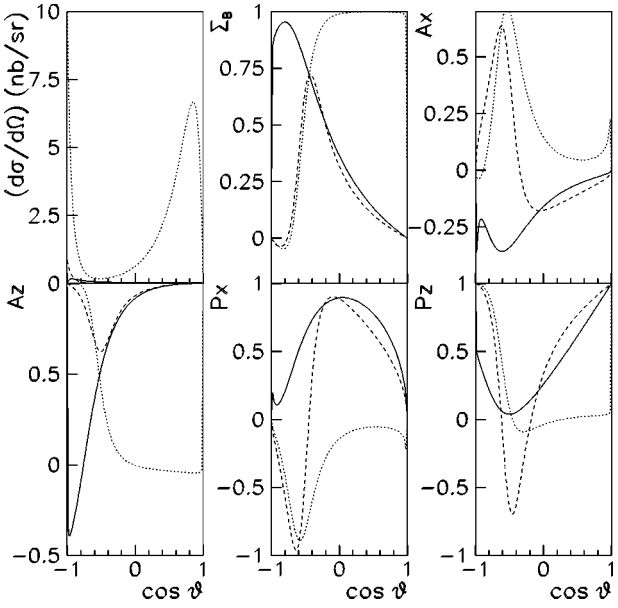

FIG. 8. Differential cross section and polarization observables Σ_B, $\mathcal{A}_x$, $\mathcal{A}_z$, $\mathcal{P}_x$, and $\mathcal{P}_z$, for the reactions $\gamma+n\to\Lambda_c^+ +D^-$ (solid line), $\gamma+n\to\Sigma_c^+ +D_c^-$ (dashed line), and $\gamma+n\to\Sigma_c^0+\overline{D}_c^0$ (dotted line), calculated for model I.

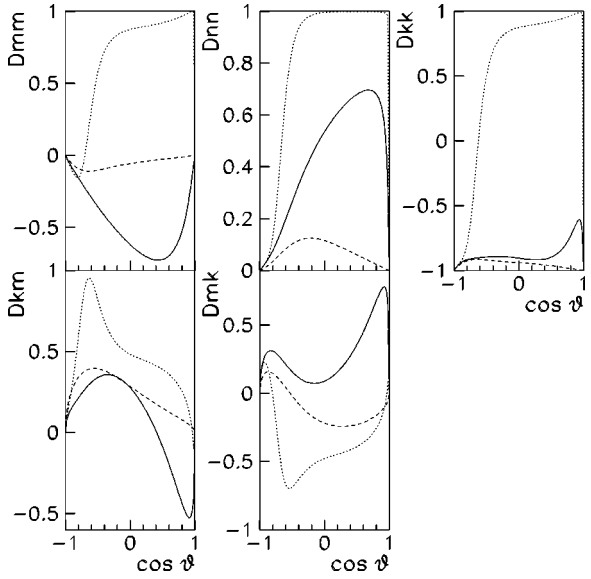

FIG. 9. Depolarization coefficients $\mathcal{D}_{ab}$ for the reactions $\gamma+p\to\Lambda_c^+ +\overline{D}_c^0$ (solid line), $\gamma+p\to\Sigma_c^{++}+D_c^-$ (dashed line), and $\gamma+p\to\Sigma_c^+ +\overline{D}_c^0$ (dotted line), calculated for model I.

$$A_{\gamma N}^{c\bar{c}}(E_\gamma)=\frac{\Delta\sigma_{\gamma N}^{c\bar{c}}}{\sigma_{\gamma N}^{c\bar{c}}}=\frac{\int_0^1 dx\Delta\sigma(\hat{s})\Delta G(x)}{\int_0^1 dx\sigma(\hat{s})G(x)}$$

$$=\frac{\int_{4m_c^2}^{2ME_\gamma} d\hat{s}\Delta\sigma(\hat{s})\Delta G(x)}{\int_{4m_c^2}^{2ME_\gamma} d\hat{s}\sigma(\hat{s})G(x)}, \qquad (17)$$

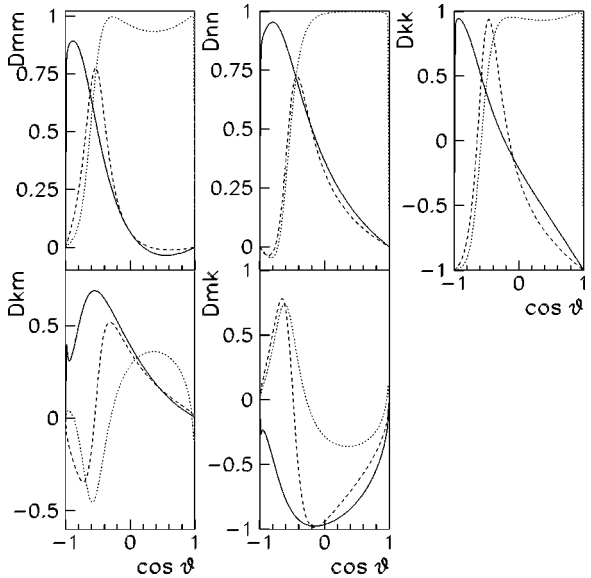

FIG. 10. Depolarization coefficients $\mathcal{D}_{ab}$ for the reactions $\gamma+n\to\Lambda_c^+ +D^-$ (solid line), $\gamma+n\to\Sigma_c^+ +D^-$ (dashed line), and $\gamma+n\to\Sigma_c^0+\overline{D}^0$ (dotted line), calculated for model I.

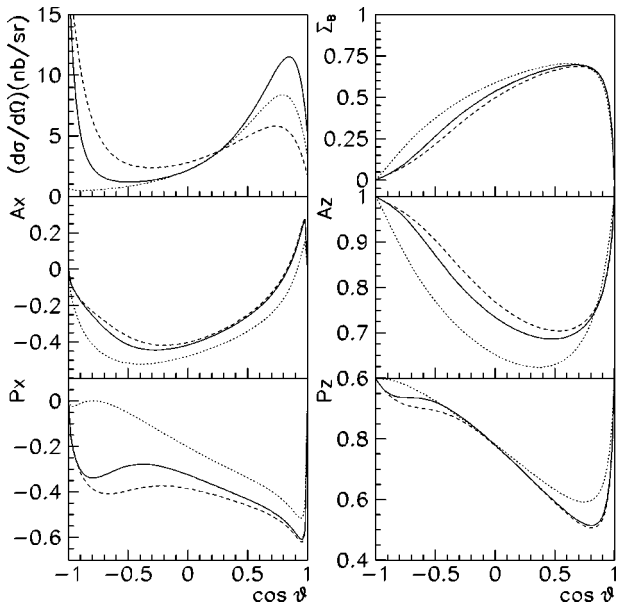

FIG. 11. $\cos\vartheta$ dependence of the differential cross section, beam asymmetry Σ_B, and polarization observables $\mathcal{A}_x$, $\mathcal{A}_z$, $\mathcal{P}_x$, and $\mathcal{P}_z$, for the reaction $\gamma+p\to\Lambda_c^+ + \bar{D}^0$ for models I (solid line), II (dashed line), and III (dotted line).

where $G(x)$ $[\Delta(G)(x)]$ is the unpolarized [polarized] gluon distribution in an unpolarized [polarized] proton, $\hat{s}$ is the square of the invariant mass of the photon-gluon system, and m_c is the charm quark mass.

Several parametrizations exist for the $G(x)$ and $\Delta G(x)$, but if the unpolarized distribution $G(x)$ is quite well constrained from the deep inelastic scattering (DIS) data and, therefore, different calculations give similar results, the polarized gluon distribution ΔG is poorly known. For illustration, $G(x)$ and $\Delta G(x)$ taken from [24] (dashed line) and from [26] model B (dotted line) and model C (dashed-dotted line) are shown in Fig. 13.

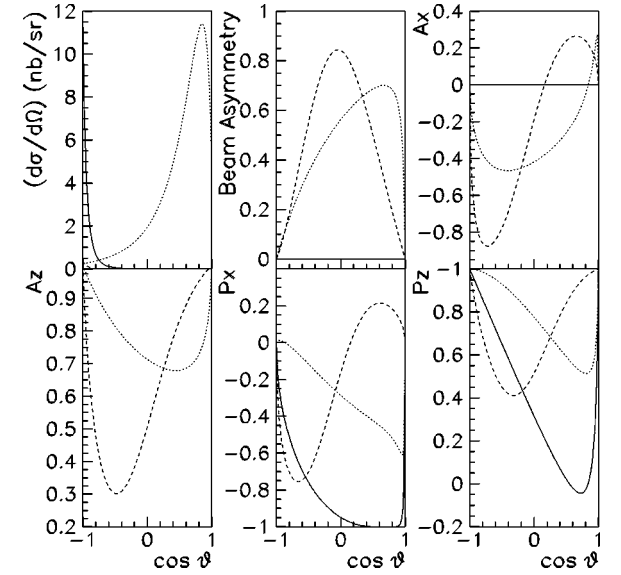

FIG. 12. $\cos\vartheta$ dependence of the different contributions to the total amplitude for the differential cross section, the beam asymmetry Σ_B, and the polarization observables $\mathcal{A}_x$, $\mathcal{A}_z$, $\mathcal{P}_x$, and $\mathcal{P}_z$, s channel (solid line), u channel (dashed line), and D^* t channel (dotted line). The first contribution gives $\Sigma_B=0$ and $\mathcal{A}_z=1$, in the entire kinematical range, because $f_{3,s}=f_{4,s}=0$.

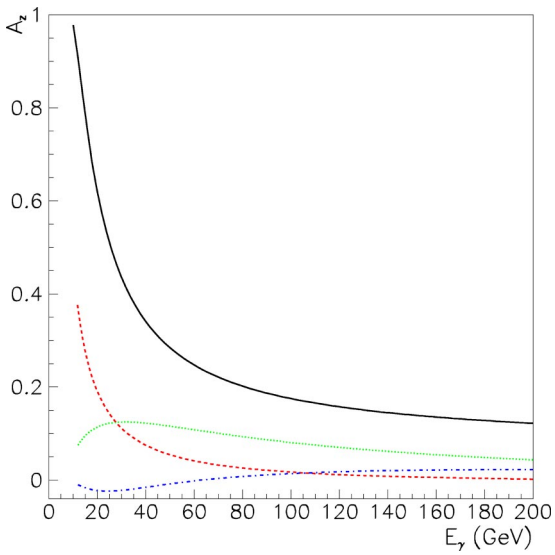

FIG. 13. Integrated $\overline{\mathcal{A}_z}(E_\gamma)$ asymmetry for the reaction $\vec{\gamma}+\vec{p}\to\Lambda_c^+ + \bar{D}_c^0$ for the ELA (solid line), for model I. Predictions for the asymmetry $A_{\gamma N}^{c\bar{c}}(E_\gamma)$ for inclusive charm photoproduction calculated with Eq. (17), taking $G(x)$ and $\Delta G(x)$ from [24] (dashed line), from [26] model B (dotted line), and from [26] model C (dash-dotted line), are also shown.

The predictions of the asymmetry $A_{\gamma N}^{c\bar{c}}(E_\gamma)$ strongly depend on the choice of $\Delta G(x)$. Moreover, the results are very sensitive to the lower limit of the integral—i.e., to m_c. The value of the charm quark mass (so called the current mass) is known from studies of the charmonium properties [35], $m_c=(1.15–1.35)$ GeV, but for the gluon distribution, values of m_c in the range $m_c=(1.5–1.7)$ GeV are more often used. In the calculations we have assumed that the fitting parameters for the functions $G(x)$ and $\Delta G(x)$ have a weak m_c dependence, and we have taken for all calculations $m_c=1.5$ GeV.

As a result of the large value of $\overline{\mathcal{A}_z}(E_\gamma)$, we can conclude that the exclusive process of associative particle production, $\gamma+p\to\Lambda_c^+ + \bar{D}^0$, has to be taken into account as possible background for the extraction of the polarized gluon distribution $\Delta G(x,Q^2)$ from the measurement of the A_z asymmetry in the inclusive process $\vec{\gamma}+\vec{N}\to\text{charm}+X$. The importance of exclusive processes $\gamma+p\to Y_c^+ + \bar{D}_c$, $\bar{D}_c^*$ in the estimation of the asymmetry A_z in open charm photoproduction has been mentioned earlier [54,55].

VI. CONCLUSIONS

We calculated the differential and total cross sections for the exclusive processes $\gamma+N\to Y_c+\bar{D}_c$. We also calculated a set of T- and P-even polarization observables, such as the Σ_B asymmetry, induced by a linearly polarized photon beam

on an unpolarized nucleon target, the asymmetries $\mathcal{A}_x$ and $\mathcal{A}_z$, in the collisions of circularly polarized photons with a polarized nucleon target, in the reaction (i.e., xz) plane, the $\mathcal{P}_x$ and $\mathcal{P}_z$ components of the Y_c polarization, in collisions of circularly polarized photons with an unpolarized target, and the depolarization coefficients, from the polarized target to the final hyperon, with an unpolarized beam.

In the framework of the effective Lagrangian approach, we suggested a model for these processes on proton and neutron targets. The gauge invariance of the charm particle electromagnetic interaction drove our choice of specific pole diagrams. The necessary parameters of the model, such as the magnetic moments of the Y_c hyperons and the strong-coupling constants (for the vertices $N\to Y_c+\bar{D}_c$ and $N\to Y_c+\bar{D}_c^*$), have been determined from SU(4) symmetry. The phenomenological FFs, which are essential ingredients in this approach, have been taken in such a way to conserve the gauge invariance of the model, for any value of the coupling constants and cutoff parameters, and for any kinematical conditions.

The parameters of the suggested model, in particular the cutoff parameters for the meson and baryon exchanges, were fixed in order to reproduce the value of the total cross section for $\gamma+p\to\Lambda_c^++\bar{D}_c^0$, at $E_\gamma=20$ GeV (the smallest energy where open charm photoproduction has been measured).

The existing experimental information does not allow one to fix uniquely the necessary parameters. Therefore, we considered three versions of the suggested model, with different sets of coupling constants and cutoff parameters, which all reproduce the cross section at $E_\gamma=20$ GeV.

We predicted the $\cos\vartheta$ dependence of different polarization observables, which are, in principle, accessible now by the running COMPASS experiment, for example.

Large isotopic effects in the energy and $\cos\vartheta$ dependence of all these polarization observables, as well as large polarization effects (in absolute value), are a general property of the considered model.

Knowledge of the coupling constants and of the cutoff parameters, which have been used in this work, enter also for any future calculations of the electroproduction of charm particles, $e^-+N\to e^-+Y_c+\bar{D}_c$, and for the photoproduction and electroproduction of charmed vector mesons, $\gamma+N\to\bar{D}_c^*+Y_c$, $e^-+N\to e^-+\bar{D^*}+Y_c$. The same constants enter also in the estimation of the $Y_c\bar{D}_c$ associative production in neutrino-nucleon collisions, induced by neutral and weak currents [56], and for the processes $\pi+N\to N+Y_c+\bar{D}_c(\bar{D}_c^*)$ and $N+N\to N+Y_c+\bar{D}_c(\bar{D}_c^*)$. All these different processes can be calculated in the framework of the ELA, in particular in the near-threshold region.

Contributing for about 10% to the total cross section of open charm photoproduction on nucleons (for $40\leqslant E_\gamma\leqslant 250$ GeV), the exclusive process $\gamma+p\to\Lambda_c^++\bar{D}_c^0$ has to be considered an important background in the interpretation of possible polarization effects in $\gamma+N\to X+$charm processes. This refers especially to the $\mathcal{A}_z$ asymmetry in $\vec{\gamma}+\vec{N}\to X+$charm, which is considered as the most direct way to measure the gluon contribution to the nucleon spin.

The smooth behavior of the total cross section as a function of the energy, for $\gamma+p\to Y_c+\bar{D}_c$, results from the spin-1 nature of the D^* exchange. If one takes into account the high-energy Regge behavior of this exchange, the energy dependence of the differential cross section is modified as

$$\frac{d\sigma}{dt}\simeq\left(\frac{s}{s_0}\right)^{2[\alpha_{D^*}(t)-1]},$$

where $\alpha_{D^*}(t)$ is the D^* Regge trajectory, and s_0 is a parameter which defines the scale.

Taking a linear parametrization $\alpha_{D^*}(t)=\alpha(0)+\alpha' t$, one can find, for the total cross section,

$$\sigma\simeq\left(\frac{s}{s_0}\right)^{2[\alpha(0)-1]}\Big/\ln\left(\frac{s}{s_0}\right).$$

Taking an oversimplified assumption [57] $\alpha(0)=\alpha_{K^*}(0)=0.35$, one finds $\sigma\simeq s^{-1.3}$. One should expect an even faster decreasing of the cross section with energy, in the case of a strong violation of SU(4) symmetry.

ACKNOWLEDGMENT

We thank the members of the Saclay group of the COMPASS Collaboration for interesting discussions and useful comments.

APPENDIX

Here we give the expressions for the scalar amplitudes f_i, $i=1$–4:

$$f_i=f_{i,s}+f_{i,u}+f_{i,t}(D)+f_{i,t}(D^*),$$

where the indices s, u, and t correspond to s-, u-, and t-channel contributions.

s channel:

$$f_{1,s}=g_{NY_cD}\frac{e}{W+m}\left[Q_N-(W-m)\frac{\kappa_N}{2m}\right],$$

$$f_{2,s}=g_{NY_cD}\frac{e}{W+m}\left[-Q_N-(W+m)\frac{\kappa_N}{2m}\right]\frac{|\vec{q}|}{E_2+M},$$

$$f_{3,s}=f_{4,s}=0.$$

u channel:

$$f_{1,u}=e\frac{g_{NY_cD}}{u-M^2}\times\left\{Q_{Y_c}(W-M)-\frac{\kappa_c}{2M}[t-m_D^2+(W-m)(W-M)]\right\},$$

$$f_{2,u}=-e\frac{g_{NY_cD}}{u-M^2}\frac{|\vec{q}|}{E_2+M}\left\{Q_{Y_c}(W+M)+\frac{\kappa_c}{2M}[t-m_D^2+(W+m)(W+M)]\right\}\frac{W-m}{W+m},$$

$$f_{3,u}=e\frac{g_{NY_cD}}{u-M^2}|\vec{q}|\frac{W-m}{W+m}\left[2Q_{Y_c}+\kappa_c\frac{W+m}{M}\right],$$

$$f_{4,u}=e\frac{g_{NY_cD}}{u-M^2}(E_2-M)\left[-2Q_{Y_c}+\kappa_c\frac{W-m}{M}\right],$$

where $W^2=s$, $E_2=(s+M^2-m_D^2)/(2W)$.

t channel (D contribution):

$$f_{1,t}(D)=f_{2,t}(D)=0,$$

$$f_{3,t}(D)=-2eQ_D\frac{g_{NY_cD}}{t-m_D^2}|\vec{q}|\frac{W-m}{W+m},$$

$$f_{4,u}(D)=2eQ_D\frac{g_{NY_cD}}{t-m_D^2}(E_2-M).$$

t channel (D^* contribution):

$$f_{1,t}(D^*)=\frac{e}{2}\mathcal{N}(g_1+g_2)[t-m_D^2+2(W-m)(W-M)]+\frac{g_2}{m+M}[-tW+mm_D^2-2(m+M)(W-m)\times(W-M)],$$

$$f_{2,t}(D^*)=e\mathcal{N}(g_1+g_2)\frac{W-m}{W+m}\frac{|\vec{q}|}{E_2+M}\times\left\{\frac{1}{2}[t-m_D^2+2(W+m)(W+M)]+\frac{g_2}{m+M}\times[tW+mm_D^2-2(m+M)(W+m)(W+M)]\right\},$$

$$f_{3,t}(D^*)=-e\mathcal{N}|\vec{q}|(W-m)\left[g_1+g_2-g_2\frac{W+m}{W-m}\right],$$

$$f_{4,t}(D^*)=-e\mathcal{N}(W-m)(E_2+M)\left[g_1+g_2+g_2\frac{W-m}{W+m}\right],$$

with

$$\mathcal{N}=\frac{g_{D^*D\gamma}}{(t-m_{D^*}^2)}\frac{1}{m_{D^*}}.$$

[1] D. Aston *et al.*, Phys. Lett. **94B**, 113 (1980).
[2] European Muon Collaboration, J.J. Aubert *et al.*, Nucl. Phys. **B213**, 31 (1983); Phys. Lett. **167B**, 127 (1986).
[3] SLAC Hybrid Facility Photon Collaboration, K. Abe *et al.*, Phys. Rev. D **33**, 1 (1986).
[4] Photon Emulsion Collaboration, M.I. Adamovich *et al.*, Phys. Lett. B **187**, 437 (1987).
[5] Tagged Photon Spectrometer Collaboration, J.C. Anjos *et al.*, Phys. Rev. Lett. **62**, 513 (1989).
[6] NA14/2 Collaboration, M.P. Alvarez *et al.*, Phys. Lett. B **246**, 256 (1990); **278**, 385 (1992); Z. Phys. C **60**, 53 (1993).
[7] L.M. Jones and H.W. Wyld, Phys. Rev. D **17**, 759 (1978); F. Halzen and D.M. Scott, Phys. Lett. **72B**, 404 (1978); H. Fritzsch and K.H. Streng, *ibid.* **72B**, 385 (1978); V.A. Novikov, M.A. Shifman, A.I. Vainstein, and V.I. Zakharov, Nucl. Phys. **B136**, 125 (1978); Yad. Fiz. **27**, 771 (1978); J. Babcock, D.W. Sivers, and S. Wolfram, Phys. Rev. D **18**, 162 (1978).
[8] M.P. Rekalo, Ukr. Phys. J. **22**, 1602 (1977).
[9] M.P. Rekalo and E. Tomasi-Gustafsson, Phys. Lett. B **500**, 53 (2001).
[10] D.W. Duke and J.F. Owens, Phys. Rev. Lett. **44**, 1173 (1980).
[11] A.D. Watson, Z. Phys. C **12**, 123 (1982); P. Ratcliffe, Nucl. Phys. **B223**, 45 (1983).
[12] COMPASS Collaboration, G. Baum *et al.*, Report No. CERN-SPSLC-96-14.
[13] H. Ohlsen and L.C. Maximon, Phys. Rev. **110**, 589 (1958).
[14] K. Aulenbacher *et al.*, Nucl. Instrum. Methods Phys. Res. A **391**, 498 (1997).
[15] Jefferson Lab Hall A Collaboration, K. Wijesooriya *et al.*, Phys. Rev. Lett. **86**, 2975 (2001).
[16] S.J. Brodsky and G.P. Lepage, Phys. Rev. D **24**, 2848 (1981).
[17] V. Ghazikhanian *et al.*, SLAC Proposal No. E161, 2000, website: http://www.slac.stanford.edu/exp/e161/
[18] Spin Muon Collaboration (SMC), D. Adams *et al.*, Phys. Lett. B **329**, 399 (1994); **339**, 332(E) (1994).
[19] Spin Muon Collaboration, D. Adams *et al.*, Phys. Lett. B **357**, 248 (1995).
[20] E143 Collaboration, K. Abe *et al.*, Phys. Rev. Lett. **74**, 346 (1995).
[21] SLD Collaboration, K. Abe *et al.*, Phys. Rev. Lett. **73**, 25 (1994).
[22] FNAL E581/704 Collaboration, D.L. Adams *et al.*, Phys. Lett. B **336**, 269 (1994).
[23] G. Bunce *et al.*, Part. World **3**, 1 (1992).
[24] S.J. Brodsky, M. Burkardt, and I. Schmidt, Nucl. Phys. **B441**, 197 (1995).
[25] M. Gluck, E. Reya, and A. Vogt, Eur. Phys. J. C **5**, 461 (1998); M. Gluck, E. Reya, M. Stratmann, and W. Vogelsang, Phys. Rev. D **63**, 094005 (2001).
[26] T. Gehrmann and W.J. Stirling, Phys. Rev. D **53**, 6100 (1996).
[27] S.J. Brodsky, E. Chudakov, P. Hoyer, and J.M. Laget, Phys. Lett. B **498**, 23 (2001).

[28] M.P. Rekalo and E. Tomasi-Gustafsson, Phys. Rev. D **65**, 014010 (2002).
[29] Z.W. Lin and C.M. Ko, Phys. Rev. C **62**, 034903 (2000) and references therein.
[30] T. Matsui and H. Satz, Phys. Lett. B **178**, 416 (1986).
[31] G.F. Chew, M.L. Goldberger, F.E. Low, and Y. Nambu, Phys. Rev. **106**, 1345 (1957).
[32] S.B. Gerasimov, Sov. J. Nucl. Phys. **2**, 430 (1966); S.D. Drell and A.C. Hearn, Phys. Rev. Lett. **16**, 908 (1967).
[33] J. Ahrens *et al.*, Phys. Rev. Lett. **84**, 5950 (2000); **87**, 022003 (2001).
[34] Jefferson Lab E94-010 Collaboration, R. Gilman, Nucl. Phys. **A689**, 445 (2001).
[35] Particle Data Group, K. Hagiwara *et al.*, Phys. Rev. D **66**, 010001 (2002).
[36] A.N. Aleev *et al.*, Sov. J. Nucl. Phys. **43**, 395 (1986); M. Jezabek, K. Rybicki, and R. Rylko, Phys. Lett. B **286**, 175 (1992).
[37] J. Smith and R. Vogt, Z. Phys. C **75**, 271 (1997).
[38] SLAC Hybrid Facility Photon Collaboration, V. O'Dell *et al.*, Phys. Rev. D **36**, 1 (1987).
[39] H. Rubinstein and L. Stodolsky, Phys. Lett. B **76**, 479 (1978).
[40] SLAC Hybrid Facility Photon Collaboration, K. Abe *et al.*, Phys. Rev. D **30**, 694 (1984).
[41] H. Haberzettl, Phys. Rev. C **56**, 2041 (1997); H. Haberzettl, C. Bennhold, T. Mart, and T. Feuster, *ibid.* **58**, 40 (1998).
[42] M.P. Rekalo and E. Tomasi-Gustafsson, Phys. Rev. C **67**, 044004 (2003) and references therein.
[43] A.M. Gasparyan, V.Y. Grishina, L.A. Kondratyuk, W. Cassing, and J. Speth, nucl-th/0210018.
[44] M.P. Rekalo and E. Tomasi-Gustafsson, Eur. Phys. J. A **16**, 575 (2003).
[45] M.P. Rekalo and E. Tomasi-Gustafsson, Phys. Rev. C **67**, 038501 (2003).
[46] M.P. Rekalo and E. Tomasi-Gustafsson, Phys. Rev. D **65**, 074023 (2002) and references therein.
[47] M.J. Savage, Phys. Lett. B **326**, 303 (1994).
[48] M. Guidal, J.M. Laget, and M. Vanderhagen, Nucl. Phys. **A627**, 645 (1997).
[49] S. Bianco, hep-ex/9911034.
[50] K. Stenson, in Proceedings of 34th Rencontres de Moriond QCD and Hadronic Interactions, Les Arcs, France, 1999.
[51] E687 Collaboration, P. Frabetti *et al.*, Phys. Lett. B **370**, 222 (1996).
[52] SELEX Collaboration, F.G. Garcia *et al.*, Phys. Lett. B **528**, 49 (2002).
[53] E791 Collaboration, E.M. Aitala *et al.*, Phys. Lett. B **495**, 42 (2000).
[54] G.K. Mallot, J. Phys. G **25**, 1539 (1999).
[55] M. Ryskin and E. Leader, J. Phys. G **25**, 1541 (1999).
[56] CHORUS Collaboration, A. Kayis-Topaksu *et al.*, Phys. Lett. B **555**, 156 (2003); **539**, 188 (2002).
[57] K.G. Boresov and A.B. Kaidalov, Sov. J. Nucl. Phys. **37**, 100 (1973).